Title

Measuring Correlated Electronic and Vibrational Spectral Dynamics Using Line Shapes in Two-Dimensional Electronic-Vibrational Spectroscopy

Authors

Lewis, Nicholas HC
Dong, Hui
Oliver, Thomas AA
et al.

Publication Date

2015

DOI

10.1063/1.4919686

Peer reviewed

Measuring Correlated Electronic and Vibrational Spectral Dynamics Using Line Shapes in Two-Dimensional Electronic-Vibrational Spectroscopy

Nicholas H. C. Lewis, Hui Dong, Thomas A. A. Oliver, and Graham R. Fleming[a)]

Department of Chemistry, University of California, Berkeley, California 94720, United States

Physical Biosciences Division, Lawrence Berkeley National Laboratory, Berkeley, California 94720, United States and

Kavli Energy Nanoscience Institute at Berkeley, Berkeley, California 94720, United States

Two-dimensional Electronic-Vibrational spectroscopy (2DEV) is an experimental technique that shows great promise in its ability to provide detailed information concerning the interactions between the electronic and vibrational degrees of freedom in molecular systems. The physical quantities 2DEV is particularly suited for measuring have not yet been fully determined, nor how these effects manifest in the spectra. In this work, we investigate the use of the center line slope of a peak in a 2DEV spectrum as a measure of both the dynamic and static correlations between the electronic and vibrational states of a dye molecule in solution. We show how this center line slope is directly related to the solvation correlation function for the vibrational degrees of freedom. We also demonstrate how the strength with which the vibration on the electronic excited state couples to its bath can be extracted from a set of 2DEV spectra. These analytical techniques are then applied to experimental data from the laser dye 3,3'-diethylthiatricarbocyanine iodide in deuterated chloroform, where we determine that lifetime of the correlation between the electronic transition frequency and the transition frequency for the backbone C=C stretch mode to be ~ 1.7 ps. Furthermore, we find that on the electronic excited state this mode couples to the bath ~ 1.5 times more strongly than on the electronic ground state.

[a)]Electronic mail: grfleming@lbl.gov

I. INTRODUCTION

Ultrafast multi-dimensional spectroscopies have been developed into highly effective techniques for studying the dynamics of molecules in condensed phases. The most prevalent of these techniques, two-dimensional electronic spectroscopy (2DES) and two-dimensional infrared spectroscopy (2DIR), are capable of characterizing the transition frequency fluctuations of electronic or vibrational degrees of freedom.[1–5] In particular, certain parameters of the lineshapes of the resulting correlation spectra, such as the ellipticity of a feature or the slope of the center line, have been shown to be directly related to the frequency-frequency correlation function for the relevant degrees of freedom.[6–9] Recently we have developed a two color spectroscopic technique that combines the advantages of electronic and vibrational spectroscopies and provides new information by correlating these disparate degrees of freedom, an experiment that we have termed 2D electronic-vibrational spectroscopy (2DEV).[10] This technique directly measures the cross peak that would occur between the 2DES and 2DIR spectra, which provides information about the coupling between the electronic and vibrational degrees of freedom.

The 2DEV experiment utilizes a sequence of three laser pulses, with controlled time delays between each interaction. The first two pulses are resonant with an electronic transition, while the third pulse is resonant with a fundamental vibrational transition. Following the first pulse the system evolves for the time period t_1 according to an electronic coherence, which encodes the initial electronic transition frequency of the system. The second pulse then causes the system to evolve according to a population, either on the excited or ground electronic state, for the waiting time t_2. During this period the system undergoes spectral diffusion by interacting with the bath and due to microscopic changes in specific solvent-solute interactions. The third pulse subsequently probes the changes that have occurred during t_2 by causing the system to once again evolve according to a coherence, which radiates the third-order signal as a function of the third time delay t_3. Because the third pulse is resonant with a vibrational transition, however, the changes that are probed are those which are directly correlated to this vibration, isolating only these components of the frequency-frequency correlation function. The signal field is measured by interfering it with a local oscillator on a spectrometer, which provides the transition frequency of the final vibrational state that results from the evolution during t_2. In typical 2DES and 2DIR experiments all

three laser pulses are degenerate, and therefore they primarily interrogate diagonal features, for which the same correlation function describes the coherence dephasing during t_1 and t_3 and the spectral diffusion during t_2, and cross peaks between nearby transitions, which typically have similar interactions with the bath. For the 2DEV experiment, the dynamics instead report on the correlation between these disparate aspects of the system.

2DEV is still a new technique, and it has shown promise by revealing simultaneous dynamics of the electronic and vibrational states following an electronic excitation, showing the dynamic Stokes shifts for both these degrees of freedom in the laser dye 4-(di-cyanomethylene)-2-methyl-6-p-(dimethylamino)styryl-4H-pyran (DCM).[10] The physical quantities 2DEV is particularly suited for measuring have not yet been fully determined, nor how these effects manifest in the spectra. In a separate paper we discuss in general terms what types of correlations in both the homogeneous and the inhomogeneous line broadening mechanisms are expected to contribute to the spectra, and show that the slope of the nodal line between the features corresponding to t_2 evolution on the electronic ground and excited states is sensitive to these correlations.[11] Here we focus on extracting quantitative information about the solvation correlation function and the strength of the coupling between the system and its bath. In this case the system is the laser dye 3,3'-diethylthiatricarbocyanine iodide (DTTCI) dissolved in deuterated chloroform ($CDCl_3$).

Specifically, we investigate the properties of a model composed of a two-level electronic system, with the ground and first excited levels of a single vibration treated explicitly on both the ground and excited electronic states. The level diagram for the model is illustrated in Figure (1.a). The electronic and vibrational degrees of freedom are allowed to interact with separate baths, each described by its own spectral density. Within this simple four-level model we will show how the component of the frequency fluctuations that is correlated between the electronic and vibrational degrees of freedom is directly related to the correlation function for the vibrational degree of freedom. This is due to the effect that fluctuations in the vibrational zero point energy on the electronic excited state has on the electronic transition. We will demonstrate that this can be directly measured via the dynamics in the center line slope of a feature in the 2DEV spectrum. Indeed, the center line slope is sensitive to both the dynamical homogeneous component of the correlations (i.e. correlations in the bath-induced fluctuations) as well as any static inhomogeneous distribution in the transition frequencies that is correlated between the electronic and vibrational degrees of freedom.

Finally, we present experimental results which demonstrate these dynamical correlations via the relaxation of the center line slope. Furthermore, we corroborate our model by showing the dynamics are the same as the vibrational dephasing time, as directly measured from the perturbed free induction decay of the vibrational coherence. The center line slope is also used to extract the strength of the coupling to the bath of the vibration on the excited electronic state relative to that of the vibration on the ground electronic state. This is a parameter that 2DEV is particularly suited to measure, and represents the unique strength of this technique in studying the coupling between electronic and vibrational degrees of freedom.

II. THEORETICAL

A. Model

We consider a simple model for a dye molecule in solution comprised of two electronic levels and one explicit vibrational degree of freedom, with these electronic and nuclear degrees of freedom each coupled to their own bath. The system will interact first with two visible fields, where we assume the visible fields excite the red edge of the electronic transition, and subsequently with an infrared field resonant with the vibrational transition. This allows us to consider only the ground and first excited vibrational levels on each electronic state. The Hamiltonain for our system, written in units such that $\hbar = 1$, is

$$\begin{aligned} H =& H_{g0} \left|g0\right\rangle \left\langle g0\right| + H_{g1} \left|g1\right\rangle \left\langle g1\right| \\ &+ H_{e0'} \left|e0'\right\rangle \left\langle e0'\right| + H_{e1'} \left|e1'\right\rangle \left\langle e1'\right| \end{aligned} \tag{1}$$

where the terms in the Hamiltonian are

$$
\begin{aligned}
H_{g0} =& \sum_{\xi} \omega_{\xi} a_{\xi}^{\dagger} a_{\xi} + \sum_{j} \nu_j b_j^{\dagger} b_j, \\
H_{g1} =& \omega_g + \sum_{\xi} \omega_{\xi} a_{\xi}^{\dagger} a_{\xi} \\
&+ \sum_{j} \nu_j \left[b_j^{\dagger} b_j + h_j \left(b_j^{\dagger} + b_j \right) \right], \\
H_{e0'} =& \epsilon_{eg} + \sum_{\xi} \omega_{\xi} \left[a_{\xi}^{\dagger} a_{\xi} + d_{\xi} \left(a_{\xi}^{\dagger} + a_{\xi} \right) \right] \\
&+ \sum_{j} \nu_j \left[b_j^{\dagger} b_j + \alpha_0 h_j \left(b_j^{\dagger} + b_j \right) \right], \\
H_{e1'} =& \epsilon_{eg} + \omega_e + \sum_{\xi} \omega_{\xi} \left[a_{\xi}^{\dagger} a_{\xi} + d_{\xi} \left(a_{\xi}^{\dagger} + a_{\xi} \right) \right] \\
&+ \sum_{j} \nu_j \left[b_j^{\dagger} b_j + \alpha_1 h_j \left(b_j^{\dagger} + b_j \right) \right].
\end{aligned}
\tag{2}
$$

Here, $a_{\xi}^{\dagger}$ and $b_j^{\dagger}$ (a_{ξ} and b_j) are the creation (annihilation) operators for the bath degrees of freedom for the electronic and vibrational modes, respectively. The constants ϵ_{eg}, ω_g and ω_e represent the transition frequencies for the electronic transition and for the 0-1 vibrational transitions on the ground and excited electronic states. The system-bath coupling is described by d_{ξ} for the electronic states and h_j for the vibration, for the ξth or jth bath modes. The parameters α_0 and α_1 characterize the strength with which the ground and first excited vibrational levels on the electronic excited state couple to the bath, scaled relative to the strength of the coupling to the bath for the vibration on the ground electronic state.

It is important to note that neither electronic nor vibrational relaxation is included.We assume that the visible field will only excite the electronic transition between the $v = 0$ vibrational levels of the probed vibration, and so the only contribution of the finite vibrational lifetime will be in its effects on the line width for the vibrational transition. If such lifetime broadening is not a major component of the vibrational line width, as expected for high frequency modes, then this approximation should not significantly affect the results. The effect of electronic relaxation will be to cause the signal to decay with waiting time t_2, which has no significant effect on the properties of the spectra that are the focus of this work.

Typically, it is convenient to reframe the system-bath coupling in terms of the spectral density, which here is given as $\mathcal{J}_e(\omega) = \sum_{\xi} d_{\xi}^2 \omega_{\xi}^2 \delta(\omega - \omega_{\xi})$ for the electronic transition, and

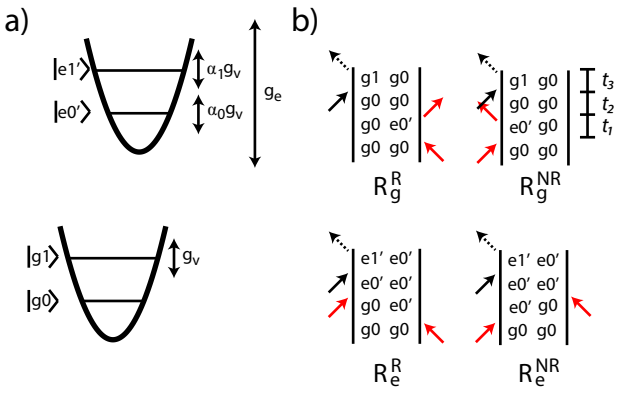

Figure 1. a) A schematic representation of the energy level structure of the hamiltonian. The states are labeled with the electronic state and the number of quanta in the vibration (here we will only allow $v = 0$ or 1). The double-headed arrows represent the bath induced fluctuations and are labeled with the line shape functions that describe how the states fluctuate relative to $|g0\rangle$ due to system-bath interactions. b) Double sided Feynman diagrams for the pathways considered in this work. The red arrows represent interactions resonant with visible photons and the black arrows represent interactions with infrared photons. The labels represent the rephasing (R^R) and nonrephasing (R^{NR}) pathways, evolving on the ground (R_g) or excited (R_e) electronic state during t_2.

likewise $\mathcal{J}_v(\omega) = \sum_j h_j^2 \nu_j^2 \delta(\omega - \nu_j)$ for the vibration. The parameters α_0 and α_1 are used to denote how the vibration-bath coupling, i.e. the spectral density $\mathcal{J}_v(\omega)$, is rescaled on the electronic excited state. Within the current model this is independent of the bath mode, and so it corresponds to a rescaling of the reorganization energy by a factor of α_0^2 and α_1^2 for the 0 and 1 vibrational levels on the electronic excited state. In general, these parameters are complicated to determine, and they likely depend on a large number of molecular parameters, such as the electronic dipole moment, the polarizability of the environment and the transition dipole of the vibration.[12,13]

In the current model we neglect explicit correlation between the fluctuations of the electronic and vibrational levels. In other words, we assume completely independent baths for these different kinds of states. In general we expect this to be a reasonable approximation, as the electronic transition will typically couple more strongly to fluctuations on a shorter time scale than vibrational transitions. A detailed consideration of explicit correlation between these degrees of freedom is beyond the scope of this work.

The response functions for this model can be derived using typical cumulant expansion methods.[11,14–16] The four Liouville pathways that are considered in this work are illustrated in Figure (1.b). The rephasing pathways are denoted $R_g^R(t_1,t_2,t_3)$, $R_e^R(t_1,t_2,t_3)$ where the subscript indicates the electronic state populated during t_2. Likewise, the nonrephasing pathways are given as $R_g^{NR}(t_1,t_2,t_3)$, $R_e^{NR}(t_1,t_2,t_3)$, and the total response is given by the sum of all four terms. They are as follows:

$$\begin{aligned}
R_g^R(t_1,t_2,t_3) &= \left\langle \mu_{eg}^2 \mu_{10}^2 \right\rangle \exp\left[i\epsilon_{eg}t_1 - i\omega_g t_3\right] \\
&\quad \times \exp\left[-g_e^*(t_1) - \alpha_0^2 g_v^*(t_1) - g_v(t_3) \right. \\
&\qquad \left. +\alpha_0 f_v^{-*}(t_1,t_2,t_3)\right], \\
R_e^R(t_1,t_2,t_3) &= -\left\langle \mu_{eg}^2 \mu_{1'0'}^2 \right\rangle \exp\left[i\epsilon_{eg}t_1 - i\omega_e t_3\right] \\
&\quad \times \exp\left[-g_e^*(t_1) - \alpha_0^2 g_v^*(t_1) - (\alpha_1-\alpha_0)^2 g_v(t_3) \right. \\
&\qquad \left. +\alpha_0(\alpha_1-\alpha_0) f_v^{+*}(t_1,t_2,t_3)\right], \\
R_g^{NR}(t_1,t_2,t_3) &= \left\langle \mu_{eg}^2 \mu_{10}^2 \right\rangle \exp\left[-i\epsilon_{eg}t_1 - i\omega_g t_3\right] \\
&\quad \times \exp\left[-g_e(t_1) - \alpha_0^2 g_v(t_1) - g_v(t_3) \right. \\
&\qquad \left. -\alpha_0 f_v^{-}(t_1,t_2,t_3)\right], \\
R_e^{NR}(t_1,t_2,t_3) &= -\left\langle \mu_{eg}^2 \mu_{1'0'}^2 \right\rangle \exp\left[-i\epsilon_{eg}t_1 - i\omega_e t_3\right] \\
&\quad \times \exp\left[-g_e(t_1) - \alpha_0^2 g_v(t_1) - (\alpha_1-\alpha_0)^2 g_v(t_3) \right. \\
&\qquad \left. -\alpha_0(\alpha_1-\alpha_0) f_v^{+}(t_1,t_2,t_3)\right],
\end{aligned} \tag{3}$$

where the auxiliary functions are defined as

$$\begin{aligned}
f^+(t_1,t_2,t_3) =& g^*(t_2) - g^*(t_2+t_3) \\
&- g(t_1+t_2) + g(t_1+t_2+t_3), \\
f^-(t_1,t_2,t_3) =& g(t_2) - g(t_2+t_3) \\
&- g(t_1+t_2) + g(t_1+t_2+t_3).
\end{aligned} \tag{4}$$

The subscripts e and v on the line shape functions indicate whether it corresponds to the electronic or vibrational degrees of freedom. The pre-factors depend on the transition dipole moment for the electronic transition μ_{eg} and for the vibrational transitions μ_{10} and $\mu_{1'0'}$ on the ground or excited electronic states, and here the angled brackets indicate orientational

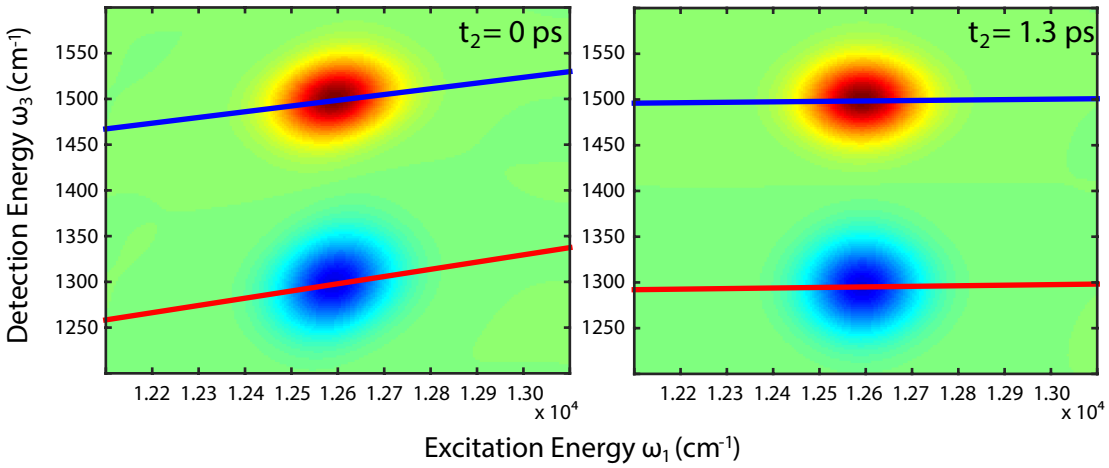

Figure 2. Simulated purely absorptive 2DEV spectra using the exact response functions in equation (3) with the center lines superimposed. The positive-going (red) features correspond to the vibration on the electronic ground state and the negative-going (blue) features correspond to the vibration on the electronic excited state. The details of this simulation are given in the text.

averaging. The line broadening functions are given by

$$\begin{aligned} g(t) = &- i\lambda t + \int_0^\infty \mathrm{d}\omega \frac{\mathcal{J}(\omega)}{\omega^2} \coth\left(\frac{\omega\beta}{2}\right)(1-\cos\omega t) \\ &+ i\int_0^\infty \mathrm{d}\omega \frac{\mathcal{J}(\omega)}{\omega^2}\sin\omega t, \end{aligned} \tag{5}$$

where $\mathcal{J}(\omega)$ is the spectral density for the electronic or vibrational degrees of freedom and β is the Boltzmann inverse temperature. The solvent reorganization energy is given by $\lambda = \int_0^\infty \mathrm{d}\omega \frac{\mathcal{J}(\omega)}{\omega}$ and is determined separately for the electronic and vibrational states by relevant spectral densities.

In the impulsive limit, the frequency domain 2D spectra $S(\omega_1, t_2, \omega_3)$ for each term in the total response function can be obtained by taking the Fourier transform over t_1 and t_3, and the total purely absorptive correlation spectrum, here referred to as S^{abp}, is obtained by combining the rephasing and nonrephasing components and taking the real part as $S^{abp}(\omega_1, t_2, \omega_3) = \mathrm{Re}\left[S^R(-\omega_1, t_2, \omega_3) + S^{NR}(\omega_1, t_2, \omega_3)\right]$. Spectra simulated using this method are shown in Figure (2). For this simulation the spectral densities are chosen to be Drude-Lorentian, which has the form $\mathcal{J}(\omega) = \frac{2\lambda\omega_c\omega}{\omega_c^2+\omega^2}$. The purpose of this simulation is not to reproduce the experimental results shown later, but to illustrate the main features of the 2DEV spectra for parameters similar to those typically used for the type of cyanine dye studied in the current experiments.[17] For the electronic degrees of freedom the cutoff

frequency $\omega_{ce} = 50$ cm^{-1} and the reorganization energy $\lambda_e = 50$ cm^{-1} and for the vibrational degrees of freedom $\omega_{cv} = 10$ cm^{-1} and $\lambda_v = 5$ cm^{-1}. The parameters scaling the strength of the coupling to the bath on the electronic excited state are set to $\alpha_0 = 0.6$ and $\alpha_1 = 1.8$, the frequency of the vibration on the ground electronic state is $\omega_g = 1500$ cm^{-1}, the frequency of the vibration on the electronic excited state is $\omega_e = 1300$ cm^{-1} and the electronic transition frequency is $\epsilon_{eg} = 12600$ cm^{-1}. The transition dipoles μ_{10} and $\mu_{1'0'}$ are taken to be the same. Of particular note is the slope of the center lines that are shown in the figure. At early t_2 the slope is positive, due to the correlation between the fluctuations of the electronic and vibrational transitions. After a few picoseconds, however, the slope decays to zero, due to the decay of the correlation function. In the following section an analytical form for the center line slope is derived.

B. Center Line Slope

The derivation is based on a short time approximation of the response for the time periods t_1 and t_3.[6–9,18] The dephasing times for the electronic coherence during t_1 and the vibrational coherence during t_3 are typically short ($\sim$ 100 fs - $\sim$ 1 ps) compared to the typical electronic population relaxation times during t_2 ($\sim$ 100 ps - $\sim$ 1 ns), so we can perform a Taylor expansion of these variables in equations (4) and (5) and truncate to second-order. Following this procedure we obtain

$$\begin{aligned} f^+(t_1,t_2,t_3) =& 2it_3\left(L^{(1)}(t_2)-\lambda\right) \\ &+ i(t_1+t_3)t_3\frac{\mathrm{d}L^{(1)}(t_2)}{\mathrm{d}t} + t_1t_3L^{(2)}(t_2), \\ f^-(t_1,t_2,t_3) =& t_1t_3\left(L^{(2)}(t_2) + i\frac{\mathrm{d}L^{(1)}(t_2)}{\mathrm{d}t}\right) \end{aligned} \tag{6}$$

and

$$g(t) = \frac{1}{2}\Omega^2t^2 \tag{7}$$

where

$$\begin{aligned} L^{(1)}(t) &\equiv \int_0^\infty \mathrm{d}\omega \frac{\mathcal{J}(\omega)}{\omega}\cos\omega t \\ L^{(2)}(t) &\equiv \int_0^\infty \mathrm{d}\omega \mathcal{J}(\omega)\coth\left(\frac{\omega\beta}{2}\right)\cos\omega t \\ \Omega^2 &\equiv \int_0^\infty \mathrm{d}\omega \mathcal{J}(\omega)\coth\left(\frac{\omega\beta}{2}\right). \end{aligned} \tag{8}$$

Here $L^{(1)}(t)$ is the solvation correlation function and Ω^2 is the mean square fluctuation of the transition frequency for the relevant degrees of freedom. The functions $L^{(1)}(t)$ and $L^{(2)}(t)$ are related by the fluctuation dissipation theorem. $L^{(1)}(t)$ describes the bath induced dissipation, and $L^{(2)}(t)$ describes the fluctuations.[19] If $L^{(1)}(t)$ is a slowly varying function, then we can neglect the terms that involve $\mathrm{d}L^{(1)}(t)/\mathrm{d}t$ and further simplify equation (6) to obtain

$$\begin{aligned} f^{+}(t_1, t_2, t_3) &= 2it_3 \left(L^{(1)}(t_2) - \lambda \right) + t_1 t_3 L^{(2)}(t_2), \\ f^{-}(t_1, t_2, t_3) &= t_1 t_3 L^{(2)}(t_2). \end{aligned} \tag{9}$$

This approximation is reasonable for the absorptive (real) part of the spectrum when the solvation correlation function is over-damped, and at high temperatures.[6] The validity of these approximations, for the parameter regime considered in this work, are illustrated with an example simulation in Figure (3).

Together, using equations (7) and (9), the response functions in equation (3) can be

simplified to

$$
\begin{aligned}
R_g^R(t_1,t_2,t_3) =& \left\langle \mu_{eg}^2 \mu_{10}^2 \right\rangle \\
& \times \exp\left[i\epsilon_{eg} t_1 - i\omega_g t_3 \right] \\
& \times \exp\left[-\frac{1}{2} A t_1^2 \right] \times \exp\left[-\frac{1}{2} B_g t_3^2 \right] \\
& \times \exp\left[-C_g(t_2) t_1 t_3 \right], \\
R_e^R(t_1,t_2,t_3) =& -\left\langle \mu_{eg}^2 \mu_{1'0'}^2 \right\rangle \\
& \times \exp\left[i\epsilon_{eg} t_1 - i\left(\omega_e + \Delta\omega_e(t_2)\right) t_3 \right] \\
& \times \exp\left[-\frac{1}{2} A t_1^2 \right] \times \exp\left[-\frac{1}{2} B_e t_3^2 \right] \\
& \times \exp\left[-C_e(t_2) t_1 t_3 \right], \\
R_g^{NR}(t_1,t_2,t_3) =& \left\langle \mu_{eg}^2 \mu_{10}^2 \right\rangle \\
& \times \exp\left[-i\epsilon_{eg} t_1 - i\omega_g t_3 \right] \\
& \times \exp\left[-\frac{1}{2} A t_1^2 \right] \times \exp\left[-\frac{1}{2} B_g t_3^2 \right] \\
& \times \exp\left[C_g(t_2) t_1 t_3 \right], \\
R_e^{NR}(t_1,t_2,t_3) =& -\left\langle \mu_{eg}^2 \mu_{1'0'}^2 \right\rangle \\
& \times \exp\left[-i\epsilon_{eg} t_1 - i\left(\omega_e + \Delta\omega_e(t_2)\right) t_3 \right] \\
& \times \exp\left[-\frac{1}{2} A t_1^2 \right] \times \exp\left[-\frac{1}{2} B_e t_3^2 \right] \\
& \times \exp\left[C_e(t_2) t_1 t_3 \right],
\end{aligned}
\tag{10}
$$

where

$$
\Delta\omega_e(t) \equiv 2\alpha_0 \left(\alpha_1 - \alpha_0\right) \left(L_v^{(1)}(t) - \lambda_v \right) \tag{11}
$$

is the dynamic Stokes shift for the vibrational transition on the electronic excited state and we have defined

$$
\begin{aligned}
A &\equiv \Omega_e^2 + \alpha_0 \Omega_v^2, \\
B_g &\equiv \Omega_v^2, \\
B_e &\equiv (\alpha_1 - \alpha_0)^2 \Omega_v^2, \\
C_g(t_2) &\equiv -\alpha_0 L_v^{(2)}(t_2), \\
C_e(t_2) &\equiv -\alpha_0(\alpha_1 - \alpha_0) L_v^{(2)}(t_2)
\end{aligned}
\tag{12}
$$

to simplify the notation. These terms correspond to the different origins of the overall

line shape, where A is the component for the electronic transition, and B_g and B_e are the pure vibrational components on the ground and excited electronic states. The most interesting terms are $C_g(t_2)$ and $C_e(t_2)$, which are the components of the line shape that are correlated between the electronic and vibrational degrees of freedom. Within the current approximations A, B_g and B_e are static components of the line shape, whereas $C_g(t_2)$ and $C_e(t_2)$ evolve with t_2, decaying proportionally to the vibrational correlation function $L_v^{(2)}(t_2)$.

The Fourier transforms over t_1 and t_3 can be performed analytically for the form of the response functions given in equation (10) to provide:

$$S_g^{abp}(\omega_1, t_2, \omega_3) = \frac{2\left\langle \mu_{eg}^2 \mu_{10}^2 \right\rangle}{\left(AB_g - \left(C_g(t_2)\right)^2\right)^{1/2}} \times \exp\left[\frac{\begin{pmatrix} -A(\omega_3 - \omega_g)^2 - B_g(\epsilon_{eg} - \omega_1)^2 \\ -2C_g(t_2)(\epsilon_{eg} - \omega_1)(\omega_g - \omega_3) \end{pmatrix}}{2AB_g - 2\left(C_g(t_2)\right)^2}\right],$$

$$S_e^{abp}(\omega_1, t_2, \omega_3) = \frac{-2\left\langle \mu_{eg}^2 \mu_{1'0'}^2 \right\rangle}{\left(AB_e - \left(C_e(t_2)\right)^2\right)^{1/2}} \times \exp\left[\frac{\begin{pmatrix} -A\left(\omega_e + \Delta\omega_e(t_2) - \omega_3\right)^2 - B_e(\epsilon_{eg} - \omega_1)^2 \\ -2C_e(t_2)(\epsilon_{eg} - \omega_1)(\omega_e + \Delta\omega_e(t_2) - \omega_3) \end{pmatrix}}{2AB_e - 2\left(C_e(t_2)\right)^2}\right]. \tag{13}$$

The complete spectrum is obtained by adding the contributions from the ground and excited electronic states.

At early t_2, the fluctuations in the electronic and vibrational degrees of freedom are correlated through the fluctuations of the vibrations on the electronic excited state. This has the effect of making the slope of the center lines of each feature non-zero. To evaluate the dynamics of the center line slopes, we can determine an analytic form as a function of t_2. To do this we differentiate the real (absorptive) part of the spectrum with respect to ω_3, which is then set to 0 and can be solved to give $\omega_g{}'$ and $\omega_e{}'$, the maxima in ω_3 as a function of ω_1, parameterized by t_2

$$\begin{aligned} \omega_g{}'(\omega_1, t_2) &= k_g(t_2)(\omega_1 - \epsilon_{eg}) + \omega_g \\ \omega_e{}'(\omega_1, t_2) &= k_e(t_2)(\omega_1 - \epsilon_{eg}) + \omega_e + \Delta\omega_e(t_2) \end{aligned} \tag{14}$$

where the slopes of the center lines are given by

$$\begin{aligned} k_g(t_2) &= \frac{\alpha_0 L_v^{(2)}(t_2)}{\Omega_e^2 + \alpha_0 \Omega_v^2}, \\ k_e(t_2) &= \frac{\alpha_0(\alpha_1 - \alpha_0) L_v^{(2)}(t_2)}{\Omega_e^2 + \alpha_0 \Omega_v^2}, \end{aligned} \tag{15}$$

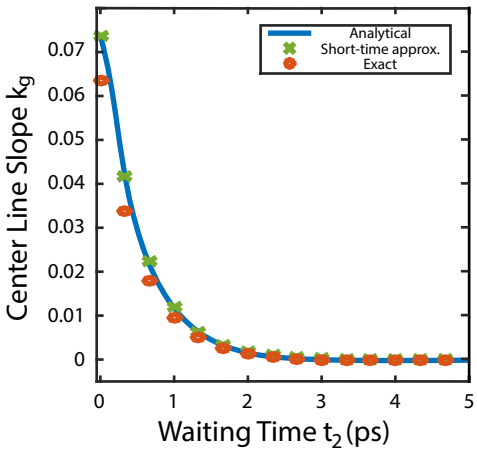

Figure 3. The center-line slope of the ground state feature for the model shown in Figure (2). The solid blue line shows the analytical result from equation (15), the green crosses show the result for the calculation with the short-time approximation without the further approximation in equation (9) and the red circles show the result for the calculation using the exact response functions in equation (3). The small discrepancy between the exact result and the analytical result comes from the relatively long vibrational dephasing and the short-time approximation. The discrepancy decreases as λ_v is increased.

and so the center line slopes for both the ground (k_g) and excited (k_e) electronic states are directly proportional to $L_v^{(2)}(t_2)$. Furthermore, we can take the ratio

$$\frac{k_e(t_2)}{k_g(t_2)} = (\alpha_1 - \alpha_0) \tag{16}$$

and therefore if it is possible to separately measure k_g and k_e for the same vibrational mode, then these can be used to provide an approximation for the strength with which the vibrational transition on the electronic excited state couples to its bath. The dynamics for the center line slope extracted from simulated spectra are shown in Figure (3) comparing the center line slope for the exact response function with the short time approximation and the analytical result in equation (15).

In the presence of inhomogeneous broadening, a result analogous to equation (16) can be obtained. To determine this we allow the transition energies ϵ_{eg}, ω_g and ω_e to be described

by a joint gaussian distribution function, such as

$$\begin{aligned} p(\epsilon_{eg}, \omega_g) = & \frac{1}{2\pi\sigma_{eg}\sigma_{\omega_g}\sqrt{1-\zeta^2}} \\ & \times \exp\left[-\frac{(\epsilon_{eg}-\epsilon_{eg}^0)^2}{2\left(1-\zeta^2\right)\sigma_{eg}^2} - \frac{(\omega_g-\omega_g^0)^2}{2\left(1-\zeta^2\right)\sigma_{\omega_g}^2}\right. \\ & \left. + \frac{\zeta(\epsilon_{eg}-\epsilon_{eq}^0)(\omega_g-\omega_g^0)}{\left(1-\zeta^2\right)\sigma_{eg}\sigma_{\omega_g}}\right] \end{aligned} \tag{17}$$

where ζ is a correlation factor between the distributions of electronic and vibrational transition frequencies that is 0 when there is no correlation, $\zeta > 0$ for positive correlation and $\zeta < 0$ for negative correlation. The widths of the inhomogeneous distribution is given by σ_{eg} for the electronic transition, and by σ_{ω_g} and σ_{ω_e} for the vibrational transitions on the ground and excited electronic states. The effects that would result in this type of correlated frequency distribution have been described theoretically,[20,21] and the effect of an inhomogeneous distribution with this form is discussed at greater length in a separate paper.[11] The effect of this inhomogeneous broadening on the spectrum can be obtained by integrating $S^{abp}(\omega_1, t_2, \omega_3)$ over this distribution, after which $\tilde{k}_g$ and $\tilde{k}_e$, the center line slopes with inhomogeneous broadening included, can be found in the same manner as before:

$$\begin{aligned} \tilde{k}_g(t_2) &= \frac{\alpha_0 L_v^{(2)}(t_2) + \zeta\sigma_{eg}\sigma_{\omega_g}}{(\Omega_e^2 + \alpha_0\Omega_v^2) + \sigma_{eg}^2}, \\ \tilde{k}_e(t_2) &= \frac{\alpha_0(\alpha_1-\alpha_0) L_v^{(2)}(t_2) + \zeta\sigma_{eg}\sigma_{\omega_e}}{(\Omega_e^2 + \alpha_0\Omega_v^2) + \sigma_{eg}^2}. \end{aligned} \tag{18}$$

The long-time slope is determined by the widths of the inhomogeneous distribution and the correlation factor, and by subtracting this component and taking the ratio of these slopes we recover the same result as in equation (16)

$$\frac{\tilde{k}_e(t_2) - \tilde{k}_e(\infty)}{\tilde{k}_g(t_2) - \tilde{k}_g(\infty)} = (\alpha_1 - \alpha_0). \tag{19}$$

If instead of taking the derivative with respect to ω_3 to find the center-line at a function of ω_1 we do the reverse, differentiating with respect to ω_1, we can find an analogous centerline slope, k', defined via the equations

$$\begin{aligned} \omega_g'(\omega_3, t_2) &= k_g'(t_2)(\omega_3 - \omega_g) + \epsilon_{eg} \\ \omega_e'(\omega_3, t_2) &= k_e'(t_2)(\omega_3 - \omega_e - \Delta\omega_e(t_2)) + \epsilon_{eg}. \end{aligned} \tag{20}$$

For one-color measurements, where the same degrees of freedom is correlated with themselves after the waiting time t_2, these slopes are equivalent. Here, because the measurement is of a cross-peak, these slopes are not directly related in this manner, and instead we can find

$$\begin{aligned}\tilde{k}'_g(t_2) &= \frac{\alpha_0 L_v^{(2)}(t_2) + \zeta\sigma_{eg}\sigma_{\omega_g}}{\Omega_v^2 \ + \sigma_{\omega_g}^2}, \\ \tilde{k}'_e(t_2) &= \frac{\alpha_0(\alpha_1-\alpha_0) L_v^{(2)}(t_2) + \zeta\sigma_{eg}\sigma_{\omega_e}}{(\alpha_1-\alpha_0)^2\,\Omega_v^2 + \sigma_{\omega_e}^2}.\end{aligned} \tag{21}$$

These slopes are somewhat less useful than their counterparts, however, because it is not possible to extract $(\alpha_1 - \alpha_0)$ as in equation (19). In the absence of correlated inhomogeneous broadening, i.e. when either the system is purely homogeneously broadened or $\zeta = 0$, if we note that $L_v^{(2)}(0) = \Omega_v^2$ then we can determine α_0 and α_1 explicitly and find them to be

$$\begin{aligned}\alpha_0 &= k'_g(0) \\ \alpha_1 &= \frac{k'_g(0)}{k'_e(0)} + k'_g(0).\end{aligned} \tag{22}$$

Therefore in certain circumstances it can be possible to directly measure the relative strengths with which the vibration couples to the bath on the excited versus the ground electronic states.

Through the derivation of equations (16) and (22) we have a general analytical procedure which can be used to extract information from 2DEV spectra about the correlated aspects of the line shape, as well as to obtain values for the important parameters α_0, α_1 and $\alpha_1 - \alpha_0$ which describe the strength of the vibrational coupling to the bath on the electronic excited state for a given vibrational mode.

III. EXPERIMENTAL

A. Methods

The experimental details involved in 2DEV have been described previously.[10] Briefly, the experiment was driven by the output of an amplified Ti:Sapphire femtosecond laser system (Coherent; Legend Elite USP; 806 nm, 40 fs, 0.9 mJ, 1 kHz). A portion of this laser (~ 0.2 mJ) was used to pump a homebuilt mid-IR optical parametric amplifier (OPA), creating 200 nJ pulses centered at 7 μm with a duration of ~ 80 fs.

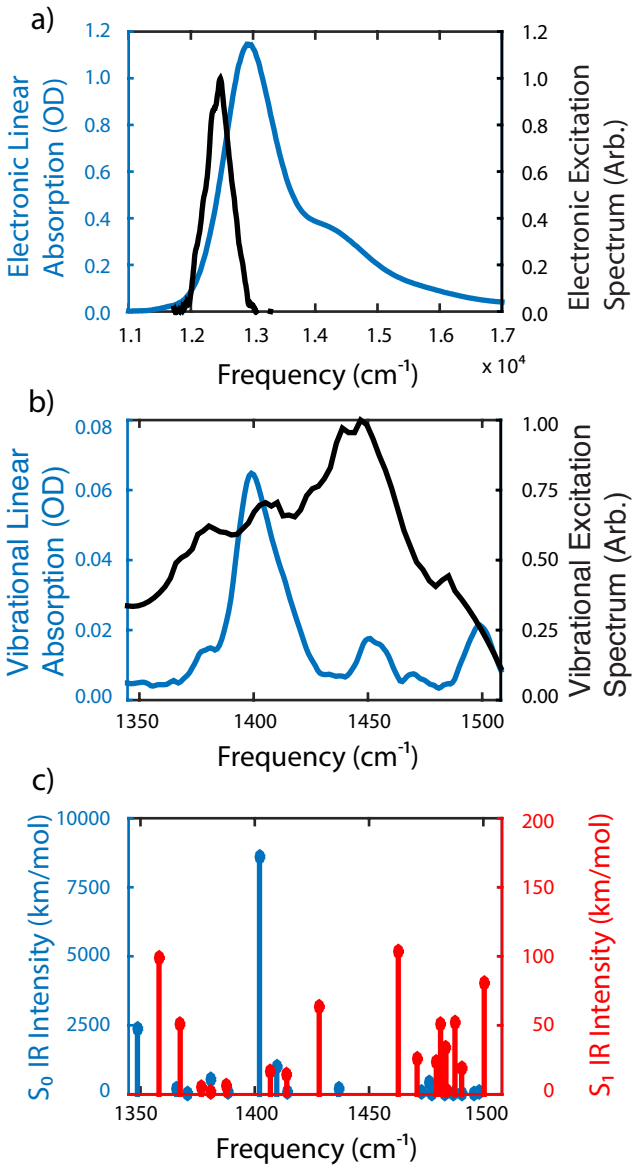

Figure 4. (a-b) The linear absorption of DTTCI dissolved in $CDCl_3$ at the concentration used in the present experiment is shown in blue. The electronic absorption is shown in a) and the vibrational absorption, with the solvent signal subtracted, is shown in b). In each case the normalized laser spectrum used to excite the relevant transition superimposed in black. c) Stick spectra of the calculated normal mode frequencies and infrared intensities within the probed region calculated for the S_0 (blue) and S_1 (red) electronic states. Note the axes for the two sets of data differ by a factor of 50. In each case the frequencies have been scaled by a factor of 0.98.[22] The details of the calculation are given in the text.

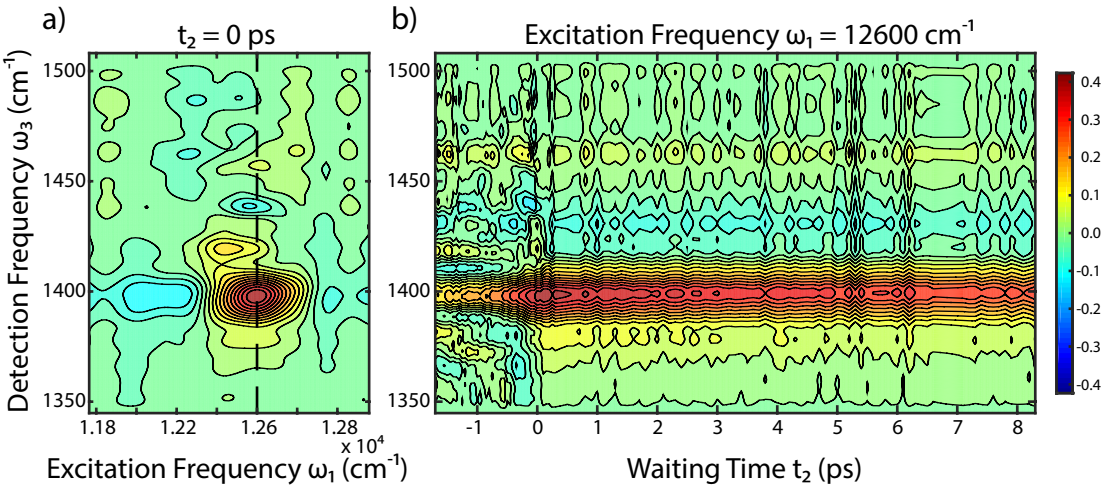

Figure 5. a) A purely absorptive 2DEV spectrum of DTTCI at $t_2 = 0$ ps. The dotted line indicates the slice through the spectrum shown as a function of t_2 in b). For $t_2 > 0$ the signal at $\omega_3 = 1400$ cm^{-1} decays with a time constant of ~ 250 ps. For $t_2 < 0$ it decays with a time constant of 1.5 ps.

The pulse pair for the electronic excitation was derived from a small portion of the regenerative amplifier beam. Prior to the sample, the pump was passed through an acousto-optic programmable dispersive filter (Fastlite; Dazzler) which was used to temporally compress the pump to 40 fs at the sample position and to generate a pair of identical pulses with a controlled time delay t_1 and relative phase ϕ_{12}. This pulse pair was then delayed by reflecting it off a retroreflector mounted on a translation stage to control the time delay t_2 between the second 800 nm pulse and the 7 μm probe pulse. At the sample, the total power of the pump beam was 100 nJ, focused to a spot size of 250 μm by an $f = 25$ cm, 90° off-axis parabolic silver mirror. The spectrum of the excitation laser at the sample position is shown in Figure (4.a).

Following the OPA, this 7 μm beam was split by a 50:50 ZnSe beam splitter to form the probe and reference beams, which were both focused at the sample to separate 250 μm spots by an $f = 15$ cm, 90° off-axis parabolic gold mirror. The probe and reference beams were then dispersed in a spectrometer (Horiba; Triax 180) and imaged onto a dual-array HgCdTe detector with 64 elements per array (Infrared Systems Development). The spectrum of the probe laser at the sample position is shown in Figure (4.b). The reference beam was used to normalize the probe spectrum, to compensate for shot-to-shot instability in the laser intensity. The probe beam was overlapped in the sample with a small portion of

the regenerative amplifier output to serve as the pump. The cross-correlation time between the pump and probe pulses was measured to be ~ 90 fs.

For each waiting time t_2 a 2DEV surface was measured by using the pulse shaper to scan the delay t_1 from 0 fs to 175 fs in 0.875 fs steps. For each value of t_1 the signal was measured with the relative phase ϕ_{12} set to 0, $\frac{\pi}{4}$, $\frac{\pi}{2}$ and $\frac{3\pi}{4}$ and the signal was recovered using a $4 \times 1 \times 1$ phase cycling scheme.[23,24] The signal was collected in the rotating frame, to remove the optical frequency of the pump from the signal. Because the experiment was performed in a partially collinear geometry (referred to as the pump-probe geometry) it was not necessary to perform a separate phasing procedure to recover the purely absorptive part of the spectrum.[25]

The sample was prepared by dissolving the laser dye DTTCI in $CDCl_3$ so that the optical density at the maximum of the electronic transition (760 nm) was 1.2 OD in a 250 μm path length cell, corresponding to 0.4 OD at the wavelength of maximum pump laser intensity (806 nm). Under these conditions $\sim 9.5\%$ of the molecules in the interaction volume were excited. The vibrational transition had an optical density of ~ 0.06. The cell was constructed from a pair of CaF_2 windows separated by a 250 μm teflon spacer, and the sample was continuously flowed to minimize the effects of local heating and photo-induced degradation of the dye. The electronic linear absorption was measured before and after the experiments to ensure the sample did not degrade over the course of the 2DEV measurements. The experiments were performed at ambient temperature. The linear absorption spectra for the electronic and vibrational transitions of the sample, with solvent subtracted, are shown in Figure (4.a) and (4.b), respectively.

B. Results

A 2DEV spectrum of DTTCI probed near 1400 cm^{-1} at $t_2 = 0$ ps is shown in Figure (5.a). The spectrum is dominated by a single positive-going feature centered at an excitation energy 12600 cm^{-1} and a detection energy of 1400 cm^{-1}. This is assigned to the bleaching of the backbone C=C stretch mode on the electronic ground state, based on density functional theory (DFT) calculations using the ωB97XD functional and the 6-311+G(d) gaussian basis set using the Gaussian09 package with a polarizable continuum solvent model with parameters appropriate for chloroform.[26] The corresponding feature for evolution of this mode

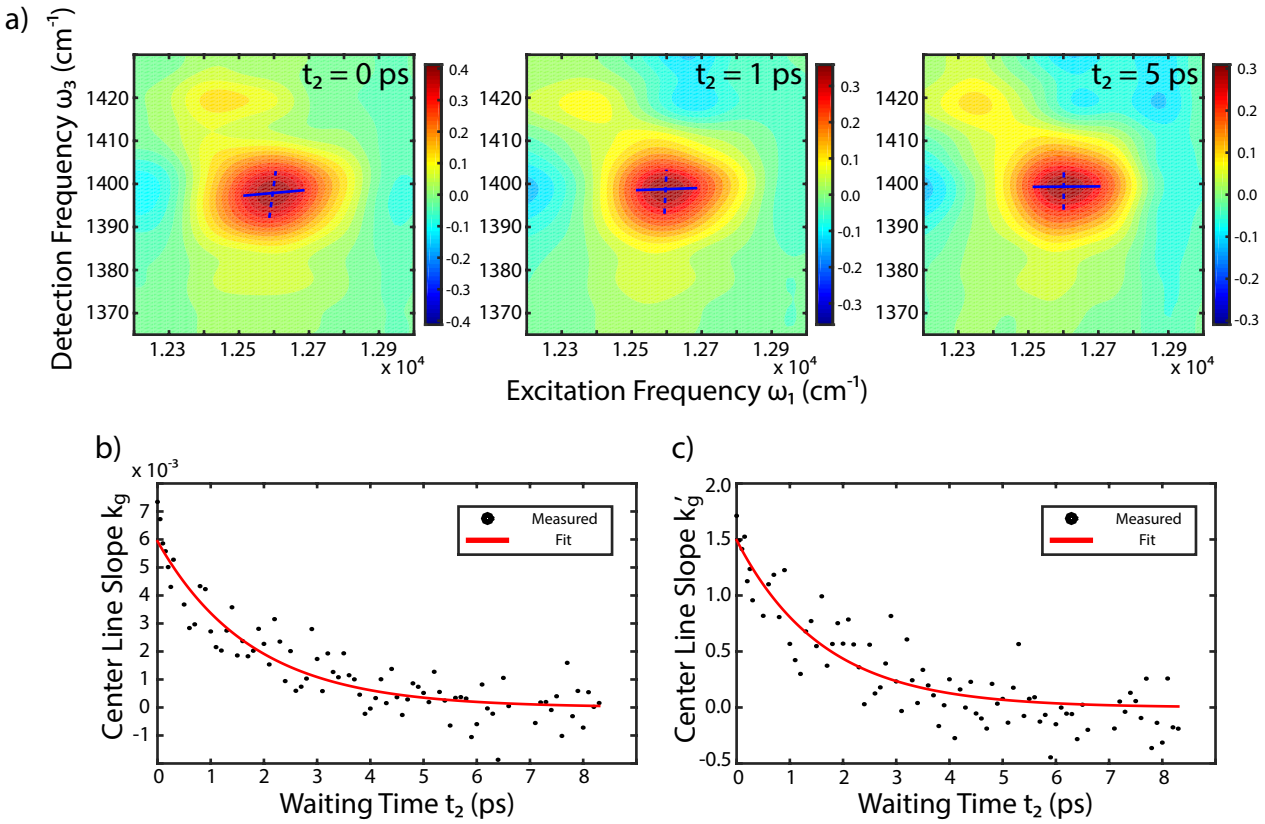

Figure 6. a) Purely absorptive 2DEV spectra of the 1400 cm^{-1} mode of DTTCI in $CDCl_3$ at waiting times $t_2 = 0$, 1 and 5 ps. The center line with respect to ω_3 is indicated by the solid lines and the center line with respect to ω_1 is indicated with dashed lines. b) The center line slope with respect to ω_3, $k_g(t_2)$, as a function of the waiting time t_2. The solid red line is the fit of the data to a single exponential, with a lifetime of $\tau = 1.8$ ps. c) The center line slope with respect to ω_1, $k'_g(t_2)$, as a function of the waiting time t_2. The solid red line is the fit of the data to a single exponential, with a lifetime of $\tau = 1.6$ ps and an amplitude of $k'_g(0) = 1.5$.

on the electronic excited state is not observed because of the very small extinction coefficient associated with the vibrational transition on the electronic excited state, as predicted from TDDFT calculations. The calculated vibrational frequencies and infrared activities are shown in Figure (4.c). The S_1 vibrations in the probed region are predicted to have activities $\sim$ 100 times smaller than the 1400 cm^{-1} S_0 mode.

In addition to the primary resonance at 1400 cm^{-1}, there are several smaller features, including two positive-going peaks, one at $\omega_3 = 1420$ cm^{-1} and the other at 1455 cm^{-1}, and a negative-going peak at $\omega_3 = 1440$ cm^{-1}. These features correspond to, respectively,

ground and excited electronic state vibrations with small vibrational oscillator strength, such as backbone C-H wag modes. Additionally there is a small amplitude negative-going peak at the same detection frequency as the primary feature but centered at a lower excitation frequency of $\omega_1 = 12100$ cm^{-1}. The origin of this peak is unclear, as it is located past the red-most edge of the DTTCI linear electronic absorption in $CDCl_3$. Due to the low intensity of these peaks the signal to noise ratio is poor, and they will not be considered further.

The dynamics of the spectrum at the frequency of the maximum absorption at $\omega_1 = 12600$ cm^{-1} is shown in Figure (5.b) as a function of detection frequency ω_3 and waiting time t_2. For $t_2 > 0$ ps the signal of the 1400 cm^{-1} mode decays with a single time constant of ~ 250 ps. This decay is substantially faster than previous studies, which have found the excited state lifetime for the S_1 state of DTTCI to be 845 ps in ethanol.[27] It is known, however, that chloroform acts as a quencher for electronic excited states,[28,29] and so the decay we observe appears to be consistent with the lifetime of the recovery of the bleach of the ground electronic state vibration, due to electronic relaxation. The central position and width of the 1400 cm^{-1} feature in the ω_3 axis does not change significantly in the first 10 ps following electronic excitation.

For $t_2 < 0$ ps, the infrared laser excites a vibrational coherence on the ground electronic state which is subsequently perturbed by the 800nm laser, and so the signal corresponds to the perturbed free-induction-decay of the vibrational coherence.[30] This signal is therefore expected to decay with the dephasing time for the vibration. It is observed that the signal intensity decays with a single time constant of 1.5 ps, providing a direct time domain measurement for the dephasing time for this vibration within the current experiment.

Of particular interest are the dynamics of the line shape of the main 1400 cm^{-1} peak. A series of 2DEV spectra at $t_2 = 0$, 1 and 5 ps is shown in Figure (6.a), focusing on the dominant feature in the spectrum. The center line slope k_g for the feature is illustrated with the solid blue lines superimposed on the spectra, while the inverse slope k_g' is shown with the dashed blue lines. To minimize potential issues with lower signal to noise ratio at the wings of the feature we only consider values greater than the half-maximum. At early t_2 the peak shows a clear ellipticity and diagonal elongation with positive center-line slopes. The decay of the center line slope k_g is shown in Figure (6.b) and the dynamics of k_g' is shown in (6.c). Here we can see that k_g has an initial value of ~ 0.006 while k_g' has an initial value of ~ 1.5.

Both slopes decay on a few picosecond timescale. They can be fit to a single exponential with lifetimes of $\tau = 1.8$ ps for k_g and 1.6 ps for k'_g, which are very close (within error) to the vibrational dephasing time found for this vibration from the perturbed free-induction decay. This agreement between the dynamics of $k_g(t_2)$ and $k'_g(t_2)$ and the vibrational dephasing time is consistent with the model Hamiltonian and equation (15). This provides support for the model discussed in this work, which predicts that these parameters should all decay with the same lifetime.

In both Figures (6.b) and (6.c) we note the slopes decay completely to 0, with no long time offset. This indicates that the 1400 cm^{-1} mode of DTTCI is either primarily homogeneously broadened, as would be expected for a dye in solution at room temperature, or that the inhomogeneous broadening is not correlated ($\zeta = 0$). In the former of these scenarios, equation (22) is applicable and we can use the fit to estimate $\alpha_0 = 1.5$, providing a direct measurement for the relative strength of the bath on the electronic excited state versus the ground state for this mode. The primary sources for error in this estimate come from the approximations made in the derivation of equations (18, 21), particularly the impulsive limit and the short time approximation. The precise effect of these approximations on the estimate for α_0 have not been fully characterized. The origin of this increase in the strength of the coupling to the bath on the electronic excited state could be explained for example by the increase in the permanent electric dipole moment – from DFT calculations the electric dipole moment increases from 1.32 D on the ground state to 1.63 D on the excited state – or other related parameters such as the polarizability.

It is interesting to note that despite analyzing a spectral feature that corresponds to t_2 evolution on the electronic ground state, it is possible to measure α_0, a parameter that describes the electronic excited state. This is because the dynamics are initiated by an electronic absorption, which depends on α_0 via its effect on the line broadening function for the electronic transition. If we also could measure the center line slope for the excited state feature corresponding to the same nuclear coordinate then it would be possible to measure α_1 for that mode in addition to α_0. If the system were inhomogeneously broadened then it would not be possible to directly measure α_0 and α_1, but only the difference. This parameter is still of interest, because it describes the strength of the coupling to the bath of the vibrational transition on the electronic excited state. 2DEV is uniquely capable of measuring these parameters, α_0 and α_1. This information would be very difficult to extract from a 2DES

spectrum, as it would be incorporated as a component of the overall electronic line shape function. In principle it might be possible to extract the $\alpha_1 - \alpha_0$ from a combination of 2DIR and transient-2DIR, but to our knowledge this has not been attempted.[31,32] Indeed, it would likely not be as straight forward as measuring the center line slopes, as these provide the normalized solvation correlation function, whereas α_1 and α_0 are related to the absolute magnitude of the coupling to the bath.

IV. CONCLUSION

In this work we have analyzed the line shape of a 2DEV resonance for a simple model comprised of a two-level electronic system with a single vibration, coupled to a bath. We make use of a short-time approximation to derive an analytical form for the center line slope of a resonance. In particular, we find that the center line slope has a decaying component which is proportional to the vibrational correlation function and a static component that depends on the correlation between the inhomogeneous frequency distributions for the electronic and vibrational transitions. The origin of the dynamic component as the vibrational correlation function comes from the effect that fluctuations in the vibrational zero point energy on the electronic excited state has on the electronic transition frequency.

In addition to the dynamics of the slope, we show that it is possible in certain circumstances to measure the relative strength of the coupling of a vibration to the bath on the electronic excited state relative to the ground state, here referred to as α_0 for the 0 vibrational level and α_1 for the first excited vibrational level. These are unique parameters that the 2DEV spectroscopic technique is particularly suitable for observing, as they are theoretically or practically excluded from being extracted from 2DES or 2DIR spectra. It may be possible to measure these parameters using transient-2DIR, but this would likely depend on a more complicated analytical procedure than that which was been presented here.

We also demonstrate experimentally the validity and practical application of the theoretical results, by showing 2DEV spectra of the 1400 cm^{-1} mode of the dye DTTCI. Here the center line slope is shown to decay with a time constant of ~ 1.7 ps, which is very close to the observed vibrational dephasing time. Furthermore, we are able to directly measure a value for α_0 for the 1400 cm^{-1} vibration of ~ 1.5. In other words, on the electronic excited state this vibration couples to the environment about 1.5 times more strongly than the electronic

ground state vibration for the same mode.

In this data we only observe the ground electronic state feature of a single vibration. An open question, therefore, is whether the parameters α_0 and α_1 vary within the same molecule for different vibrational modes. Exactly what molecular parameters these values depend on also remains uncertain, and will require further theoretical developments.

ACKNOWLEDGMENTS

The authors would like to thank Akihito Ishizaki for useful discussions. This work was supported by the National Science Foundation (NSF) under Contracts CHE-1012168 and CHE-1362830, the Director, Office of Science, Office of Basic Energy Sciences, US Department of Energy under Contract DE-AC02-05CH11231, and the Division of Chemical Sciences, Geosciences and Biosciences Division, Office of Basic Energy Sciences through Grant DE-AC03-76F000098 (at Lawrence Berkeley National Laboratory and University of California, Berkeley). We are also grateful to the College of Chemistry Molecular Graphics facility, which we used to perform our DFT calculations; this facility is funded by NSF under Contract CHE-0840505.

REFERENCES

[1]J. D. Hybl, A. Albrecht Ferro, and D. M. Jonas, J. Chem. Phys. **115**, 6606 (2001).

[2]T. Brixner, T. Mancal, I. V. Stiopkin, and G. R. Fleming, J. Chem. Phys. **121**, 4221 (2004).

[3]M. Khalil, N. Demirdöven, and A. Tokmakoff, J. Phys. Chem. A **107**, 5258 (2003).

[4]P. Hamm, M. Lim, W. F. DeGrado, and R. M. Hochstrasser, Proc. Natl. Acad. Sci. U.S.A. **96**, 2036 (1999).

[5]J. Zheng, K. Kwak, J. Asbury, X. Chen, I. R. Piletic, and M. D. Fayer, Science **309**, 1338 (2005).

[6]K. Kwac and M. Cho, J. Phys. Chem. A **107**, 5903 (2003).

[7]S. T. Roberts, J. J. Loparo, and A. Tokmakoff, J. Chem. Phys. **125**, 084502 (2006).

[8]K. Kwak, S. Park, I. J. Finkelstein, and M. D. Fayer, J. Chem. Phys. **127**, 124503 (2007).

[9]K. Kwak, D. E. Rosenfeld, and M. D. Fayer, J. Chem. Phys. **128**, 204505 (2008).

[10]T. A. A. Oliver, N. H. C. Lewis, and G. R. Fleming, Proc. Natl. Acad. Sci. U.S.A. **111**, 10061 (2014), also see corrections on Page 16628.

[11]H. Dong, N. H. C. Lewis, T. A. A. Oliver, and G. R. Fleming, (2015), submitted to J. Chem. Phys.

[12]A. Leggett, S. Chakravarty, A. Dorsey, M. Fisher, A. Garg, and W. Zwerger, Rev. Mod. Phys. **59**, 1 (1987).

[13]A. Nitzan, *Chemical Dynamics in Condensed Phases*, Relaxation, Transfer, and Reactions in Condensed Molecular Systems (Oxford University Press, 2006).

[14]S. Mukamel, *Principles of Nonlinear Optical Spectroscopy* (Oxford University Press, 1995).

[15]M. Cho, *Two-Dimensional Optical Spectroscopy* (CRC Press, 2009).

[16]P. Hamm and M. T. Zanni, *Concepts and Methods of 2D Infrared Spectroscopy* (Cambridge University Press, 2011).

[17]S. A. Passino, Y. Nagasawa, T. Joo, and G. R. Fleming, J. Phys. Chem. A **101**, 725 (1997).

[18]A. Piryatinski and J. L. Skinner, J. Phys. Chem. B **106**, 8055 (2002).

[19]Y. Tanimura, J. Phys. Soc. Jpn. **75**, 082001 (2006).

[20]M. Cho, J. Chem. Phys. **118**, 3480 (2003).

[21]S. Ham, J.-H. Kim, H. Lee, and M. Cho, J. Chem. Phys. **118**, 3491 (2003).

[22]I. M. Alecu, J. Zheng, Y. Zhao, and D. G. Truhlar, J. Chem. Theory Comput. **6**, 2872 (2010).

[23]J. A. Myers, K. L. Lewis, P. F. Tekavec, and J. P. Ogilvie, Opt. Express **16**, 17420 (2008).

[24]Z. Zhang, K. L. Wells, E. W. J. Hyland, and H.-S. Tan, Chem. Phys. Lett. **550**, 156 (2012).

[25]S. M. Gallagher Faeder and D. M. Jonas, J. Phys. Chem. A **103**, 10489 (1999).

[26]M. J. Frisch, G. W. Trucks, H. B. Schlegel, G. E. Scuseria, M. A. Robb, J. R. Cheeseman, G. Scalmani, V. Barone, B. Mennucci, G. A. Petersson, H. Nakatsuji, M. Caricato, X. Li, H. P. Hratchian, A. F. Izmaylov, J. Bloino, G. Zheng, J. L. Sonnenberg, M. Hada, M. Ehara, K. Toyota, R. Fukuda, J. Hasegawa, M. Ishida, T. Nakajima, Y. Honda, O. Kitao, H. Nakai, T. Vreven, J. A. Montgomery Jr, J. E. Peralta, F. o. Ogliaro, M. J. Bearpark, J. Heyd, E. N. Brothers, K. N. Kudin, V. N. Staroverov, R. Kobayashi, J. Normand, K. Raghavachari, A. P. Rendell, J. C. Burant, S. S. Iyengar, J. Tomasi, M. Cossi, N. Rega, N. J. Millam, M. Klene, J. E. Knox, J. B. Cross, V. Bakken, C. Adamo, J. Jaramillo,

R. Gomperts, R. E. Stratmann, O. Yazyev, A. J. Austin, R. Cammi, C. Pomelli, J. W. Ochterski, R. L. Martin, K. Morokuma, V. G. Zakrzewski, G. A. Voth, P. Salvador, J. J. Dannenberg, S. Dapprich, A. D. Daniels, Ã. d. n. Farkas, J. B. Foresman, J. V. Ortiz, J. Cioslowski, and D. J. Fox, "Gaussian 09," (2009), Gaussian Inc. Wallingford CT.

[27]C. A. Guarin, J. P. Villabona-Monsalve, R. López-Arteaga, and J. Peon, J. Phys. Chem. B **117**, 7352 (2013).

[28]E. J. Bowen, Trans. Faraday Soc. **50**, 97 (1954).

[29]W. R. Ware and C. Lewis, J. Chem. Phys. **57**, 3546 (1972).

[30]P. Hamm, Chem. Phys. **200**, 415 (1995).

[31]J. Bredenbeck, J. Helbing, and P. Hamm, J. Am. Chem. Soc. **126**, 990 (2004).

[32]M. S. Lynch, K. M. Slenkamp, M. Cheng, and M. Khalil, J. Phys. Chem. A **116**, 7023 (2012).

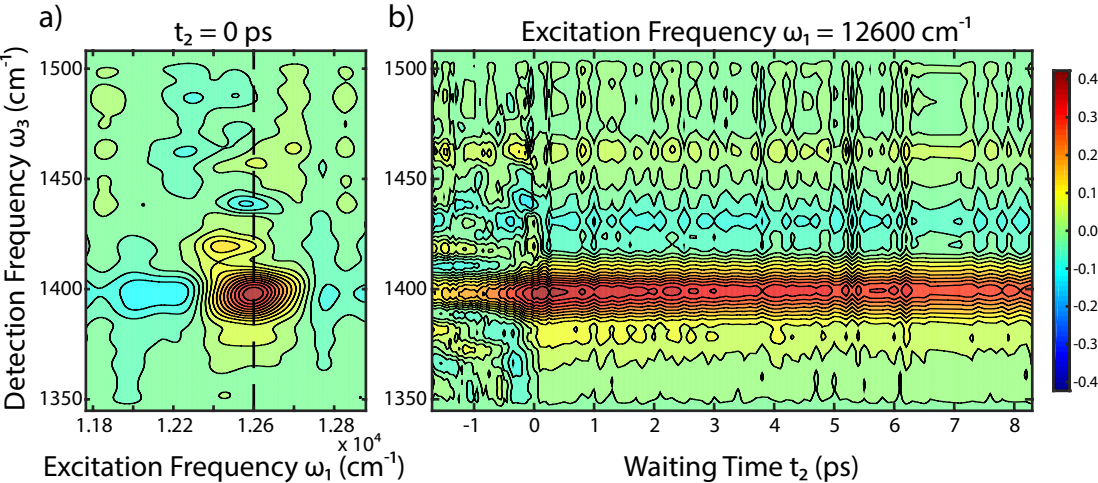
a)
t_2 = 0 ps
b)
Excitation Frequency ω_1 = 12600 cm^{-1}
Detection Frequency ω_3 (cm^{-1})
1500
1450
1400
1350
1.18
1.22
1.26
1.28
x 10^4
Excitation Frequency ω_1 (cm^{-1})
-1
0
1
2
3
4
5
6
7
8
Waiting Time t_2 (ps)
0.4
0.3
0.2
0.1
0.0
-0.1
-0.2
-0.3
-0.4

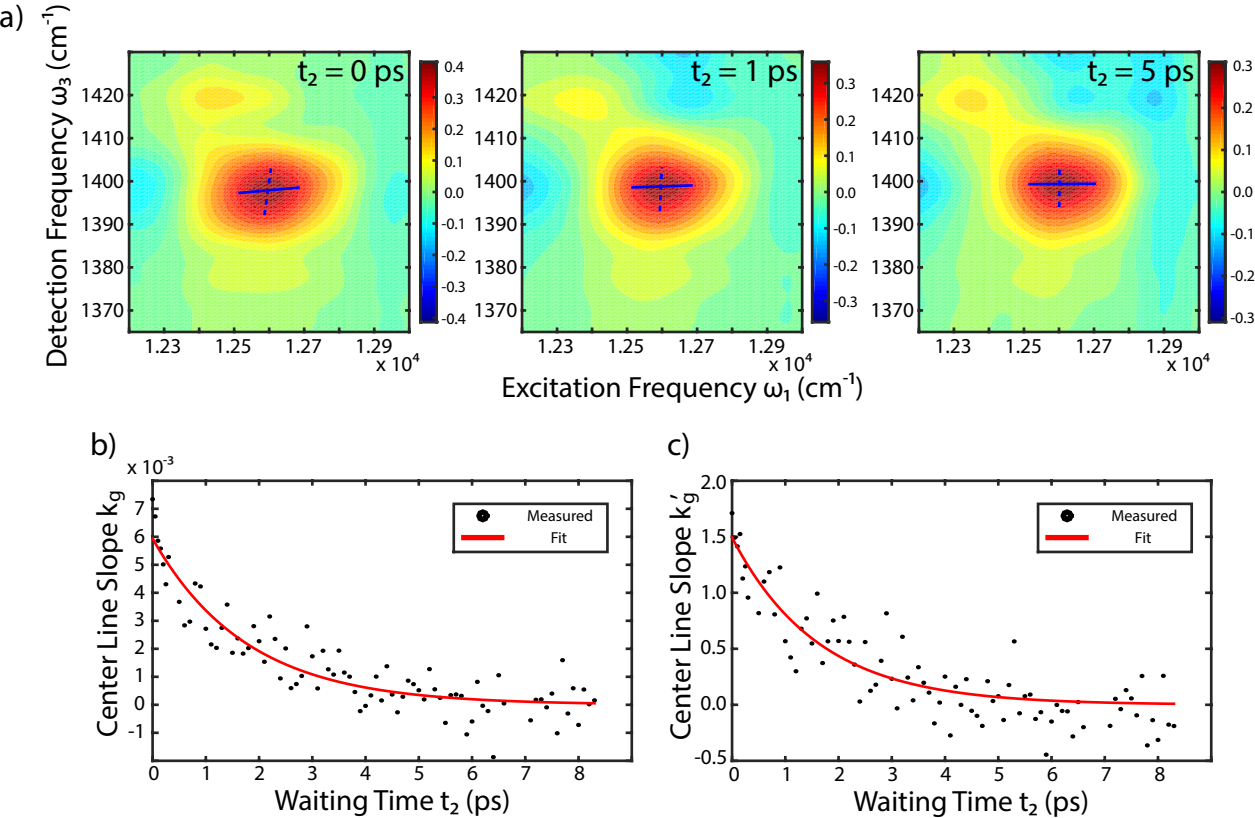
a)
$t_2 = 0$ ps
$t_2 = 1$ ps
$t_2 = 5$ ps
Detection Frequency ω_3 (cm^{-1})
Excitation Frequency ω_1 (cm^{-1})
x 10^4
b)
Center Line Slope k_g
x 10^{-3}
Measured
Fit
Waiting Time t_2 (ps)
c)
Center Line Slope k_g'
Measured
Fit
Waiting Time t_2 (ps)

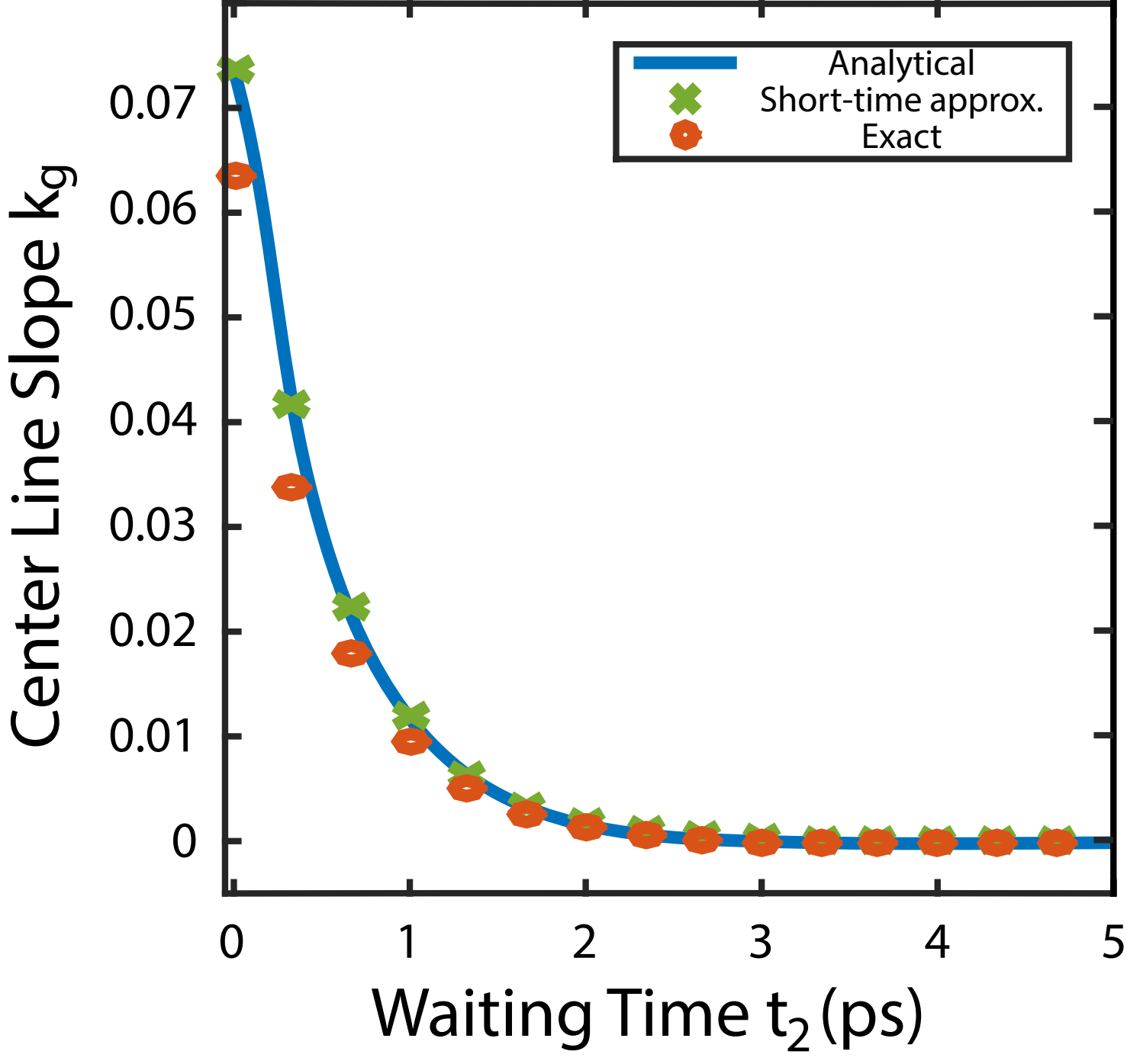
Analytical
Short-time approx.
Exact
Center Line Slope k_g
0.07
0.06
0.05
0.04
0.03
0.02
0.01
0
0
1
2
3
4
5
Waiting Time t_2 (ps)

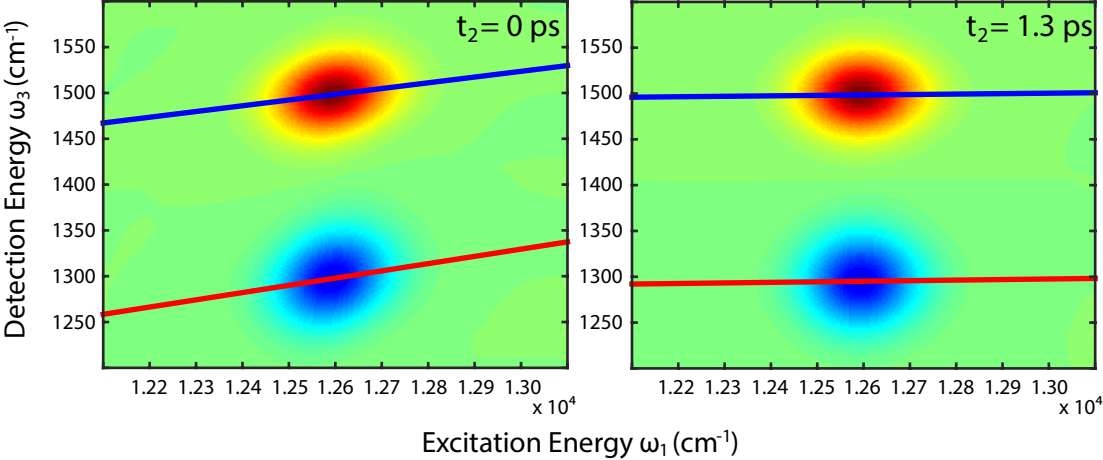
t2= 0 ps
t2= 1.3 ps
Detection Energy ω3 (cm-1)
Excitation Energy ω1 (cm-1)
1550
1500
1450
1400
1350
1300
1250
1.22 1.23 1.24 1.25 1.26 1.27 1.28 1.29 1.30
x 10^4

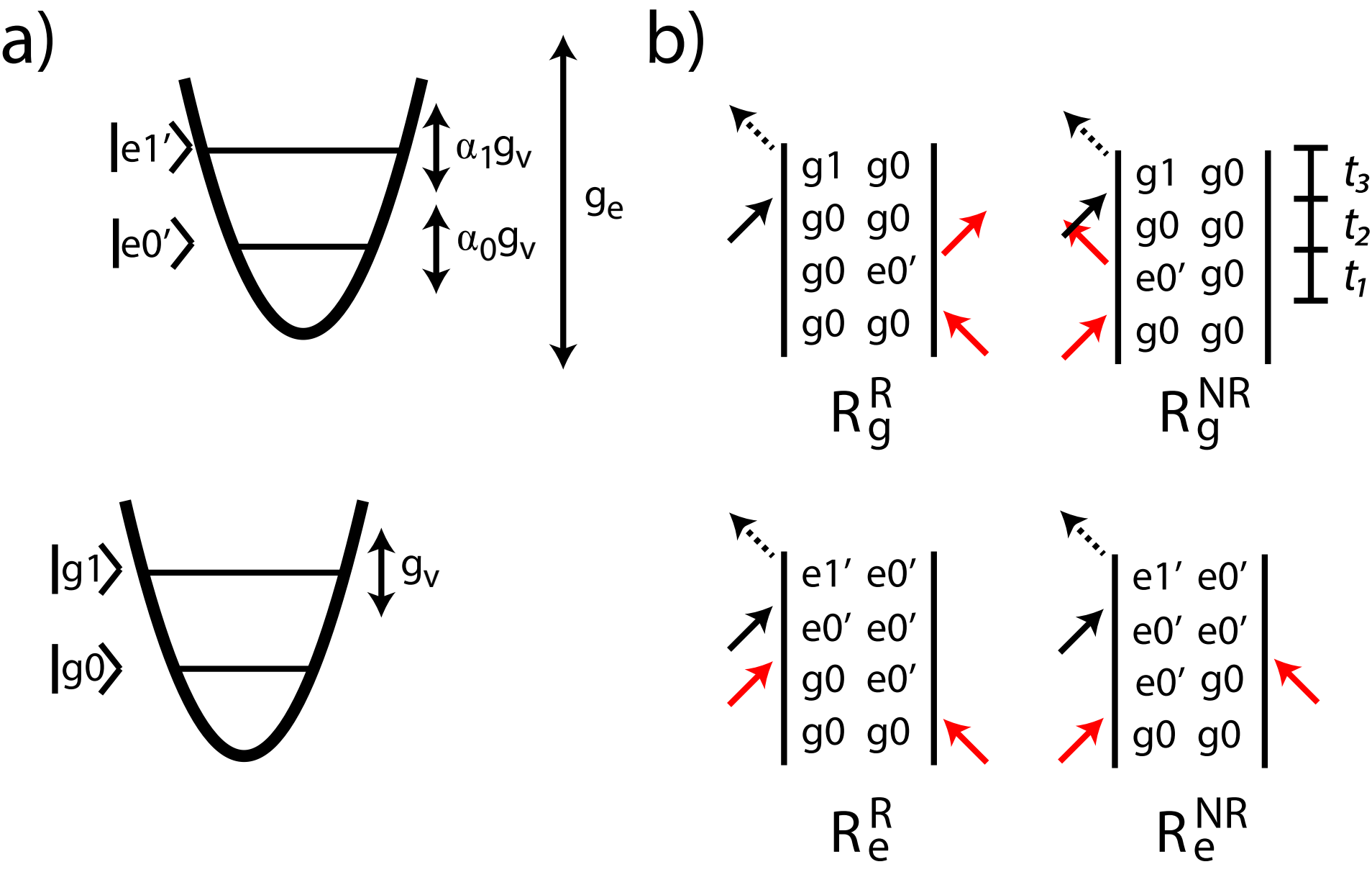
a)
|e1′⟩
|e0′⟩
α1gv
α0gv
ge
|g1⟩
|g0⟩
gv
b)
g1 g0
g0 g0
g0 e0′
g0 g0
R_g^R
g1 g0
g0 g0
e0′ g0
g0 g0
t3
t2
t1
R_g^NR
e1′ e0′
e0′ e0′
g0 e0′
g0 g0
R_e^R
e1′ e0′
e0′ e0′
e0′ g0
g0 g0
R_e^NR

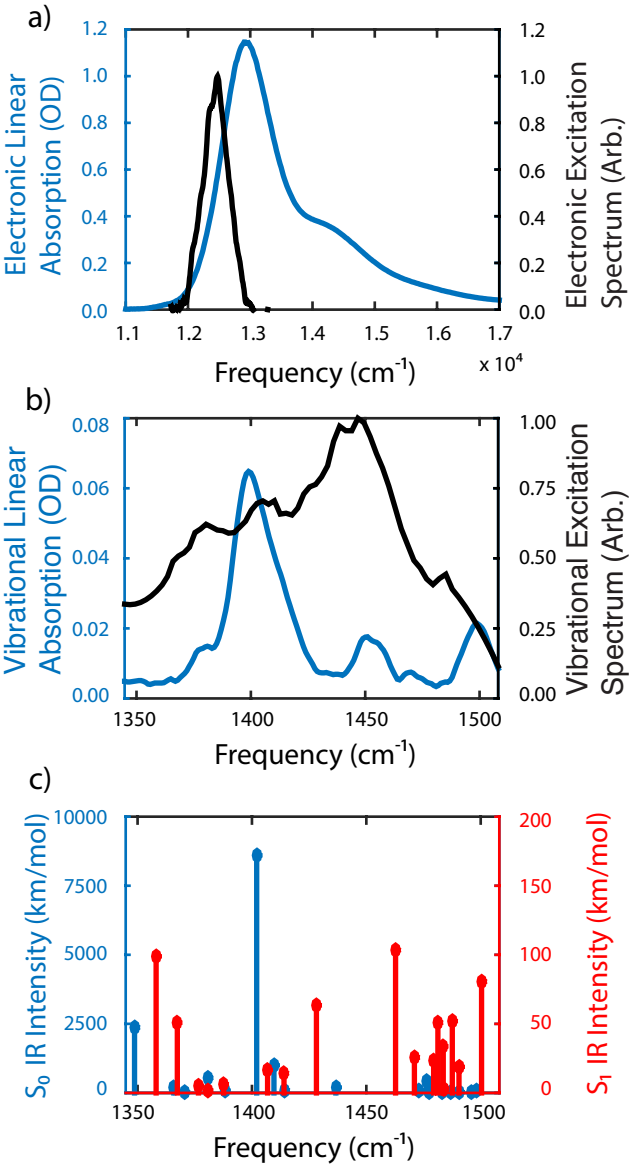
a)
Electronic Linear Absorption (OD)
Electronic Excitation Spectrum (Arb.)
Frequency (cm-1)
x 10^4
b)
Vibrational Linear Absorption (OD)
Vibrational Excitation Spectrum (Arb.)
Frequency (cm-1)
c)
S0 IR Intensity (km/mol)
S1 IR Intensity (km/mol)
Frequency (cm-1)